Ultra-broadband modulation instability gain characteristics in As_2S_3 and As_2Se_3 chalcogenide glass photonic crystal fiber*

He-Lin Wang(王河林)†, Bin Wu(吴彬), and Xiao-Long Wang(王肖隆)

Center for Optics and Optoelectronics Research, Zhejiang University of Technology, Hangzhou 310023, *China*

(Received 23 November 2015; revised manuscript received 12 January 2016; published online 20 April 2015)

Based on the designed As_2Se_3 and As_2S_3 chalcogenide glass photonic crystal fiber (PCF) and the scalar nonlinear Schrödinger equation, the effects of pump power and wavelength on modulation instability (MI) gain are comprehensively studied in the abnormal dispersion regime of chalcogenide glass PCF. Owing to high Raman effect and high nonlinearity, ultra-broadband MI gain is obtained in chalcogenide glass PCF. By choosing the appropriate pump parameter, the MI gain bandwidth reaches 2738 nm for the As_2Se_3 glass PCF in the abnormal-dispersion region, while it is 1961 nm for the As_2S_3 glass PCF.

Keywords: ultra-broadband modulation instability, Raman effect, high nonlinearity, chalcogenide glass photonic crystal fiber

PACS: 42.65.Sf, 42.65.Wi **DOI:** 10.1088/1674-1056/25/6/064207

1. Introduction

Chalcogenide glass photonic crystal fibers (PCFs) have aroused the particular interest of researchers due to high nonlinearities and lower transmission losses in the mid-infrared (MIR) regime.[1] Among them, two glass PCFs based on As_2Se_3 and As_2S_3 chalcogenide glass offer the most superior optical properties and show quite a wide range of applications in the medical, military, sensing areas[2] and optical signal procession.[3] The chalcogenide As_2Se_3 and As_2S_3 glass are transparent at MIR wavelengths as long as 10 μm,[4] and they potentially allow the generation of significant supercontinuum (SC) emission beyond 6 μm, which is high desirable for the variant advanced MIR spectral and optical applications.[5]

As far as the nonlinear effects are concerned, high Raman response plays an essential role in a four-wave mixing (FWM) process, SC generation, and wavelength conversion scheme based on cross-phase modulation (XPM), and can be used to develop Raman amplifier and Raman laser.[6,7] Besides, its high nonlinearity (n_2 is almost 100–1000 times as high as that of silica at 1.55 μm[8]) has led to the demonstrations of high speed, all optical signal processing in a compact, planar waveguide geometry for next generation optical communications systems.[9] From our previous work,[10–12] one can know that modulation instability (MI) gain depends on Raman effect and nonlinearity of fiber, while the As_2Se_3 and As_2S_3 chalcogenide glass PCFs have high Raman gains and high nonlinearities. Therefore, the effects of high Raman scattering and high nonlinearity on MI gain in the As_2Se_3 and As_2S_3 glass PCFs are a worthwhile research topic.

In this paper, with the obtained MI gain expression from the scalar nonlinear Schrödinger equation (NLSE), we will give a detailed description for MI gain characteristics including the dependences on pump wavelength and power in the As_2Se_3 and As_2S_3 glass PCFs, and mainly discuss their gain bandwidths and gain amplitudes.

2. Modulation instability gain theory for chalcogenide glass photonic crystal fiber

For non-birefringence photonic crystal fiber, the light propagation characteristic can be described with the scalar NLSE. Considering all nonlinear phenomena such as fiber dispersion, self-phase modulation (SPM), self-steepening (SS), stimulated Raman scattering (SRS), and four-wave mixing (FWM) , the NLSE is generally expressed as[13]

$$\frac{\partial U(z,t)}{\partial z}+\frac{\alpha}{2}U(z,t)+DU(z,t) = \mathrm{i}\gamma T\left(U(z,t)\int_{-\infty}^{\infty}R(\tau)\,|U(z,t-\tau)|\,\mathrm{d}\tau\right), \quad (1)$$

where $U(z,t)$ is the electric field amplitude, z is the longitudinal coordinate along the fiber, t is the time in a reference frame travelling with the pump light ω_p, $D(t)=\sum\beta_n(\mathrm{i}^{n-1}/n!)(\partial^n/\partial t^n)$, $(n\geq 2)$, and $T(t)=1+(\mathrm{i}/\omega)(\partial/\partial t)$ are the time-dependence nonlinear operator, $\beta_n=\partial^n\beta(\omega)/\partial\omega^n|\omega=\omega_\mathrm{p}$ is the nth-order frequency dependence dispersion coefficient at the central frequency of the pump pulse, $\gamma=n_2\omega_\mathrm{p}/cA_\mathrm{eff}$ is the nonlinear coefficient, n_2 is the nonlinear refractive index of chalcogenide glass, and A_eff is the effective mode area of the fiber which depends on fiber parameters such as the core radius and the core-cladding in-

*Project supported by the National Natural Science Fundation of China (Grant No. 11404286), the Natural Science Fundation of Zhejiang Province, China (Grant No. LY15F050010), and the Scientific Research Foundation of Zhejiang University of Technology, China (Grant No. 1401109012408).

†Corresponding author. E-mail: whl982032@163.com

© 2016 Chinese Physical Society and IOP Publishing Ltd

dex difference, α is the fiber loss, which is low and can be ignored.[14–17]

Using the undepleted-dump approximation method, MI can be studied by adding small perturbations into the steady solution $U_{\rm st}(z) = (P_{\rm p})^{1/2}\exp({\rm i}\gamma P_{\rm p} z)$ of Eq. (1), where $P_{\rm p}$ is the pump power. Thus, the real solution of Eq. (1) can be expressed by $U(z) = U_{\rm st}(z) + u_{\rm s}(z)\exp({\rm i}\Omega t)\exp({\rm i}\gamma P_{\rm p} z) + u_{\rm as}(z)\exp(-{\rm i}\Omega t)\exp({\rm i}\gamma P_{\rm p} z)$, where $u_{\rm s}(z)$ and $u_{\rm as}(z)$ are the small signal amplitudes of the Stokes and anti-Stokes waves at detuning frequency $\pm\Omega$, respectively, and $\Omega = \omega_{\rm p} - \omega_{\rm s} = \omega_{\rm as} - \omega_{\rm p} (\Omega > 0)$. Inserting $U(z)$ into Eq. (1), two coupled linear ordinary differential equations on the perturbations $u_{\rm s}(z)$ and $u_{\rm as}(z)$ are obtained by picking out the Stokes term and the complex conjugate of the anti-Stokes term, and making them linearized. They can be written as

$$\begin{aligned}\frac{\rm d}{{\rm d}z}\begin{pmatrix} u_{\rm s}(z) \\ u^*_{\rm as}(z)\end{pmatrix} &= {\rm i}\begin{pmatrix} a_{11} & a_{12} \\ a_{21} & a_{22}\end{pmatrix}\begin{pmatrix} u_{\rm s}(z) \\ u^*_{\rm as}(z)\end{pmatrix} \\ &= {\rm i}M^{2\times 2}\begin{pmatrix} u_{\rm s}(z) \\ u^*_{\rm as}(z)\end{pmatrix}, \end{aligned} \tag{2}$$

where $M^{2\times 2}$ denotes the stability matrix of the system. Suppose that $u_{\rm s}(z) \propto \exp(-{\rm i}\eta z)$ and $u^*_{\rm as}(z) \propto \exp(-{\rm i}\eta z)$ constitute a solution of Eq. (2), then MI occurs when η possesses a nonzero imaginary part. The perturbation parameter η depends on the pump wavelength, the pump power and the fiber parameters (including the fiber dispersion and the fiber nonlinear coefficient), and is determined by the eigenvalues of the matrix $M^{2\times 2}$. Generally, the MI gain coefficient is defined as $g_{\rm MI}(\Omega) = 2|{\rm Im}(\eta)|$, thus it is easy to obtain

$$\begin{aligned} g_{\rm MI}(\Omega) &= 2{\rm Im}\{\gamma P_P \xi R(\Omega) \pm [D(\Omega)^2 + 2\gamma P_P R(\Omega) D(\Omega) \\ &\quad + \gamma^2 P_P^2 \xi^2 R^2(\Omega)]^{1/2}\}, \end{aligned} \tag{3}$$

where $P_{\rm p}$ is the pump power, $D(\Omega) = \sum \beta_{2n}\Omega^{2n}/(2n)!$ $(n \geq 1)$ is the sum of the even order dispersion coefficients; Ω is the detuning frequency, $\Omega = \omega_{\rm p} - \omega_{\rm s} = \omega_{\rm as} - \omega_{\rm p}$ $(\Omega > 0)$, with $\omega_{\rm p}$ being the angle frequency of pump light, while $\omega_{\rm as}$ and $\omega_{\rm s}$ being the angle frequencies of the generated anti-Stokes and Stokes waves in the PCF; $\xi = \Omega/\omega_{\rm p}$; $R(\Omega)$ is the Fourier transform of Raman response function $R(t)$, whose values are different for the As_2Se_3 and As_2S_3[14–17] glass PCFs, respectively. For the chalcogenide glass, the nonlinear index can be estimated by using the explicit Kramers–Kronig transformation equation.[18] Figure 1 shows the calculated Raman susceptibilities and Raman gain spectra of As_2Se_3 and As_2S_3 glass. It is obvious that the detuning frequencies of their Raman gain peaks are 7 THz (the corresponding detuning angle frequency is $2\pi \times 7 = 43.96$ THz) and 10 THz (the corresponding detuning angle frequency is $2\pi \times 10 = 62.8$ THz). Moreover, their Raman gain frequency bandwidths are almost the same and equal to about 10 THz (the corresponding detuning angle frequency bandwidth is $2\pi \times 10 = 62.8$ THz).

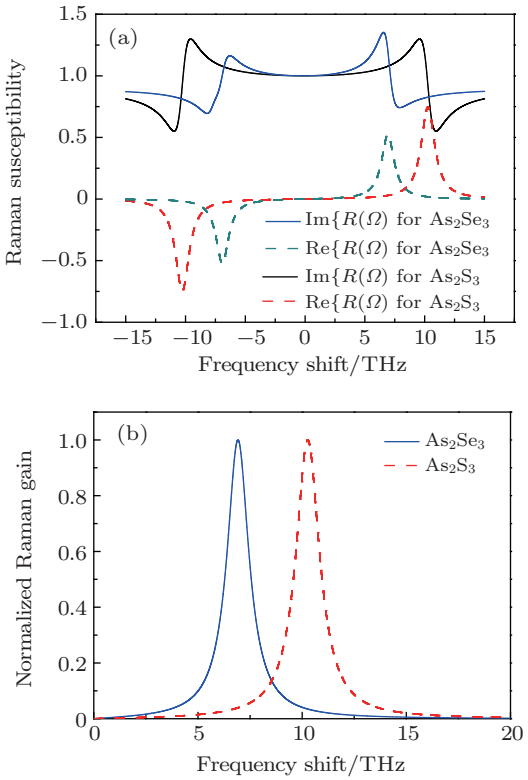


Fig. 1. (color online) Raman susceptibilities and normalized Raman gain spectral of As_2S_3 and As_2Se_3 glass.

3. Design of chalcogenide glass PCF and related parameters

For analyzing the MI gain property of the chalcogenide glass PCF, we first design PCFs each with a hexagonal geometry and five layers of air holes for optimal studies. The transverse structures and fundamental mode energy distributions of As_2Se_3 and As_2S_3 PCFs are shown in Fig. 2(a), respectively. Their air-hole diameter d =1.2 μm and the air-hole pitch Λ = 3 μm, which are the two important parameters that control the dispersions and the nonlinear coefficients of the designed PCFs. The ratio of the hole diameter to pitch is set to be $d/\Lambda = 0.4$, so that the fundamental mode can be found in the MIR (2 μm–10 μm). Background refractive index is defined by their Sellemier formula,[14,16] whose values are different for the As_2Se_3 and As_2S_3 PCFs. Based on the full-vector solver COMSOL, by using the perfect-electric-conductor boundary condition and dividing the fiber cross-sectional surface into over 10^5 non-uniform mesh grids, the effective refractive index of the fundamental mode of fiber is first calculated. Then, we can use the effective index to obtain their total dispersions in the spectral range from 2 μm to 7 μm (see Fig. 2(b)), which include the waveguide dispersion and material dispersion. It is easy to see from Fig. 2(b) that, the zero dispersion wavelengths of As_2Se_3 and As_2S_3PCFs are 3722 nm and 2908 nm, respectively. Moreover, their nonlinear coefficients are also gained from the mode field distribution (see Fig. 2(c)), which are higher than that of fused silica PCF.

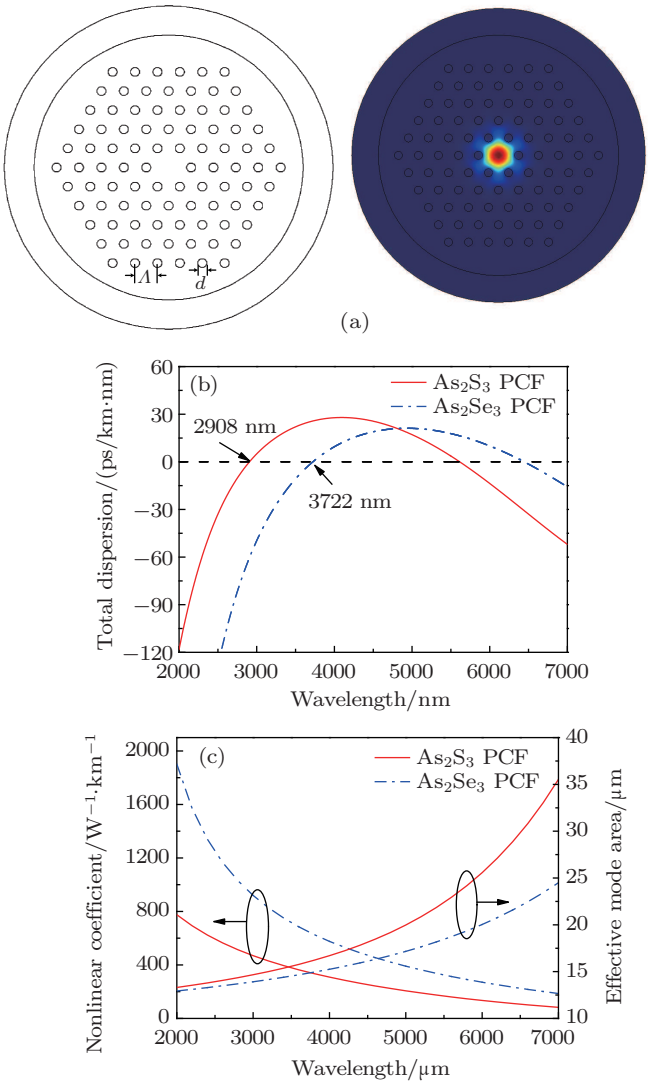


Fig. 2. (color online) Parameters of the designed As_2Se_3 PCF and As_2S_3 PCF: (a) transverse structure and field distribution; (b) dispersion variation with wavelength; (c) effective mode area and nonlinear coefficient versus wavelength.

4. MI gain characteristic

Figure 3 shows the MI gain variations with angular detuning frequency Ω in the abnormal dispersion regimes of As_2S_3 and As_2Se_3 PCFs when pump wavelength is increased and pump power $P_p = 100$ W. It can be seen from Fig. 3 that for the As_2Se_3 PCF, there are two gain spectral bands in the anti-Stokes region ($\omega_{as} > \omega_p$) or the Stokes region ($\omega_s < \omega_p$) (see Figs. 3(a) and 3(c)), while only a gain bandwidth appears in the Stokes or anti-Stokes region for the As_2S_3 PCF (see Figs. 3(b) and 3(d)). Moreover, two gain bands gradually move closer to each other in the Stokes or anti-Stokes region for the As_2Se_3 PCF when the pump wavelength varies from 3724 nm to 3748 nm (see Figs. 3(a) and 3(c)), while the single gain peak moves away from the zero angular detuning frequency point ($\Omega = 0$) for the As_2S_3 PCF (see Figs. 3(b) and 3(d)) by changing pump wavelength from 2910 nm to 2934 nm. By further analyzing Fig. 3, one can also find that, when pump wavelength moves away from their zero dispersion wavelengths (3722 nm for As_2Se_3 PCF, 2908 nm for As_2S_3 PCF) and Raman effect is considered, their gain spectral peaks gradually move away from pump wavelength. Moreover, comparing Fig. 3(a) and 3(b) with Figs. 3(c) and 3(d) respectively, one can see that the gain magnitude per meter fiber length is smaller with considering the Raman effect than without considering the Raman effect. Also, the gain magnitude per meter fiber length remains constant (see Figs. 3(a) and 3(b)) when the Raman effect is not considered. It indicates that Raman scattering makes part of the pump energy transferred into that of Raman frequency component. In fact, the phenomenon can also be obtained from the variation of the small spectral peak close to the zero detuning frequency (see the green (dotted line) boxes in Fig. 3(c) and 3(d)) because the detuning frequencies corresponding to these small peaks just lie in the Raman gain band ranges of As_2Se_3 and As_2S_3 glass (see Fig. 1(b)). Besides those results mentioned above, it should also be noted that although the MI gain peaks move with the pump wavelength variation, their MI gain bandwidths are almost equal. Therefore, the variation of pump wavelength almost has little or no influence on the MI gain bandwidth when pump power is a constant. However, the smooth degrees of these gain spectra mainly depend on the pump wavelength, and they gradually become smoother with the pump wavelength decreasing, and the reason is that the Raman gain effect disappears when pump wavelength is decreased to a value beyond the Raman gain regions of As_2Se_3 and As_2S_3 material.

Although MI gain bandwidth does not quite depend on the pump wavelength in the abnormal dispersion region for each of the As_2Se_3 and As_2Se_3 PCF, pump power may have an important effect on the MI gain bandwidth. Figure 4 shows the variations of sideband wavelength with pump power. To better express the MI gain magnitude, a color bar is used to represent the normalized MI gain value. Analyzing Fig. 4, we find that the influence of pump power on MI gain bandwidth is very obvious. For the As_2Se_3 PCF, the MI gain bandwidth gradually increases when pump power $P_p < 1000$ W, while it gradually decreases for $P_p > 1000$ W (see Fig. 4(a)), which indicates that there is an optimal pump power. For the As_2S_3 PCF, the MI gain bandwidth gradually increases with the increase of pump power (see Fig. 4(b)). Moreover, their gain bandwidths in the Stokes sideband are much larger than in the anti-Stokes sideband for the As_2Se_3 and As_2S_3 PCF. Further comparing Fig. 4(a) with Fig. 4(b), it is easy to see that the total MI gain bandwidth is much larger in the As_2Se_3 PCF than in the As_2S_3 PCF when pump power $P_p < 1600$ W, which

may be related to the high nonlinearity of the As_2Se_3 PCF. Especially for the As_2Se_3 PCF, if $P_p < 600$ W, a two-peak gain profile appears in the Stokes sideband. When $P_p > 600$ W, the two gain peaks merge together into an ultra-broadband gain profile in the Stokes sideband (see Fig. 4(a)). Similar results cannot be observed in the As_2S_3 PCF.

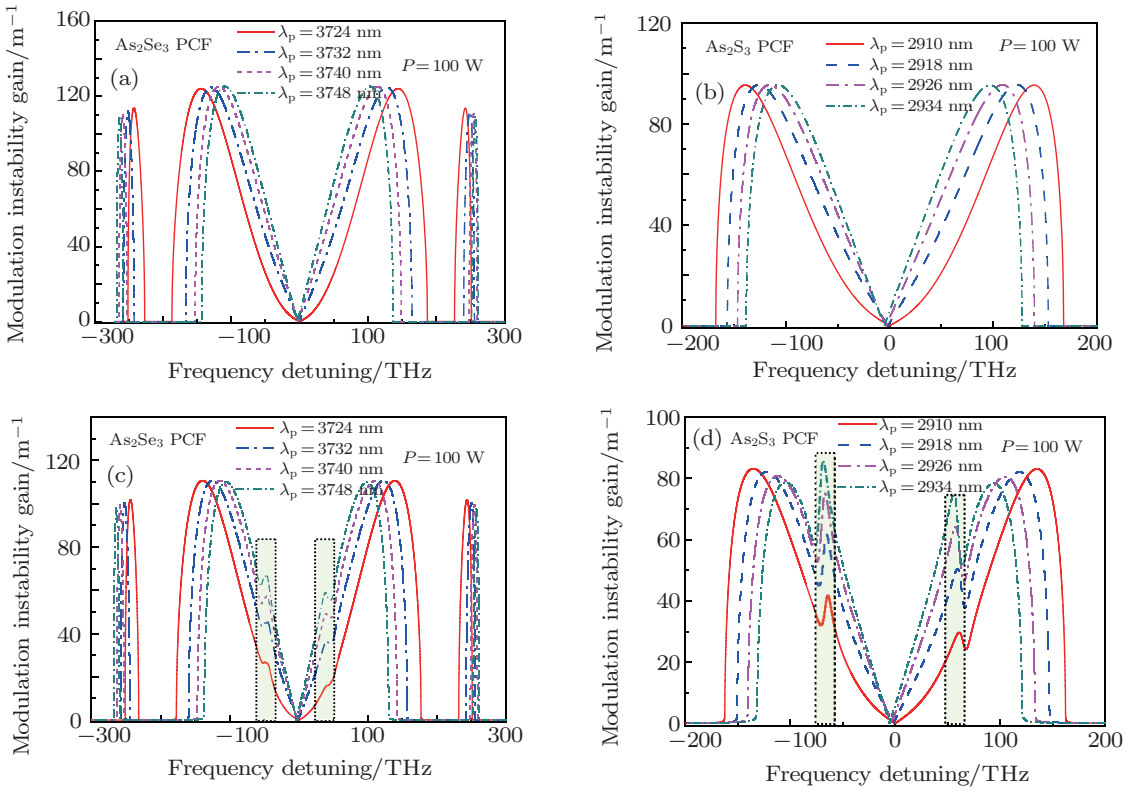


Fig. 3. (color online) MI gain variations with detuning frequency Ω in the abnormal dispersion regimes of As_2Se_3 and As_2S_3 PCF when pump wavelength is increased and pump power $P_p = 100$ W without ((a) and (b)) and with ((c) and (d)) considering Raman effect.

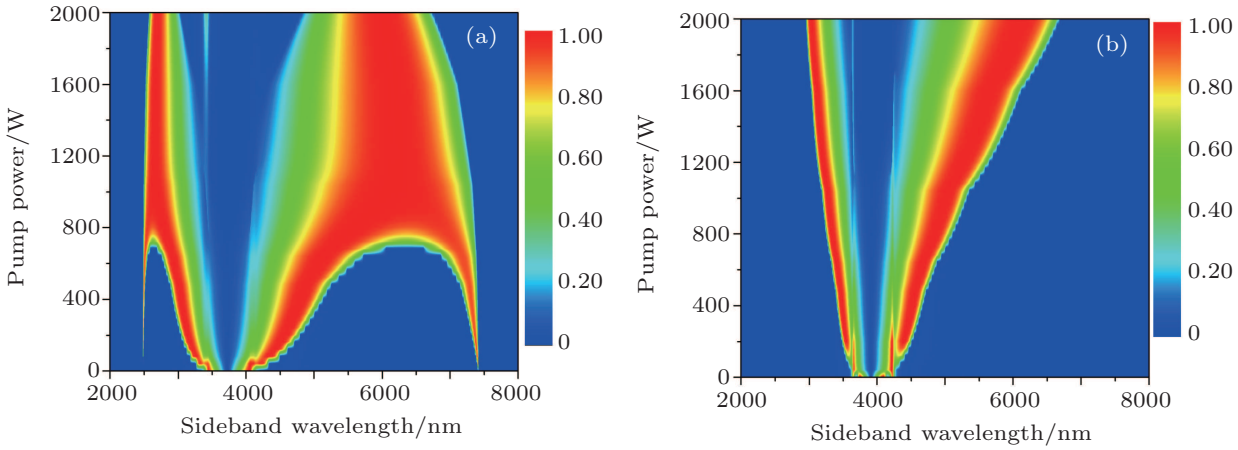


Fig. 4. (color online) Variations of sideband wavelength with pump power when pump wavelength is 3724 nm for the As_2Se_3 PCF (a), and 2910 nm for the As_2S_3 PCF (b).

Based on the above analysis, in order to achieve the smooth and ultra-broadband MI gain, pump wavelengths should be chosen to be close to their zero dispersion wavelengths (2910 nm for the As_2S_3 PCF, and 3724 nm for the As_2Se_3 PCF), while pump powers may be set to be about 700 W for the As_2Se_3 PCF and 2000 W for the As_2S_3 PCF respectively. Figure 5 shows the obtained ultra-broadband MI gain spectra in the chalcogenide glass PCFs. For the As_2Se_3 PCF, the optimal MI gain bandwidth reaches 2738 nm (498 nm + 2240 nm, see Fig. 5(a)), while it reaches 1961 nm (400 nm + 1561 nm, see Fig. 5(b)) for the As_2S_3 PCF. As far as MI gain bandwidth is concerned, the ultra-broadband gain is first gained, which is larger than that in the fused silica PCF.[11,12] Moreover, for the As_2Se_3 PCF, the gain amplitude is 500 m^{-1}, while it reaches 1600 m^{-1} for the As_2S_3 PCF. They are much larger in the chalcogenide glass PCFs. These results show that the chalcogenide glass PCFs can be used to amplify the continuous spectra based on the MI gain principle.

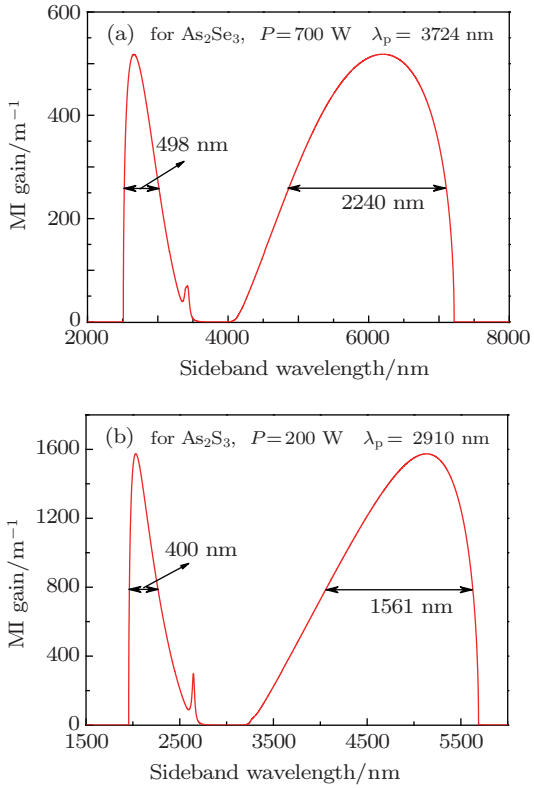


Fig. 5. (color online) Optimal ultra-broadband MI gains in the chalcogenide glass As_2Se_3 and As_2S_3 PCF.

5. Conclusions

In this work, we design the chalcogenide glass As_2Se_3 and As_2S_3 PCF, and calculate their MI gain spectra. The results indicate that it is possible to gain an ultra-broadband gain by using the chalcogenide glass As_2Se_3 and As_2S_3 PCF with the high nonlinearity and high Raman effect. By designing some special structure PCFs and choosing appropriate pump wavelength and power, the MI gain bandwidths of the As_2Se_3 and As_2S_3 PCF reach 2738 nm and 1961 nm respectively, which is the first time to use MI characteristic to obtain a ultra-broadband spectral gain structure. These findings may be used in the communication and optical amplification fields in the future.

References

[1] Sanghera J S and Aggarwal I D 1999 *J. Non-Cryst. Solids* **256–257** 6
[2] Alexander C Judge, Stephen A Dekker, Ravi Pant, Martijn de Sterke C and Benjamin J Eggleton 2010 *Opt. Express* **18** 14960
[3] Van Erps J, Luan F, Pelusi M, Iredale T, Madden S, Choi D Y, Bulla D, Luther-Davies B, Thienpont H and Eggleton B 2010 *J. Lightwave Technol.* **28** 209
[4] Weiblen R J, Docherty A, Hu J and Menyuk C R 2010 *Opt. Express* **18** 26666
[5] Ung B and Skorobogatiy M 2010 *Opt. Express* **18** 8647
[6] Shailendra K Varshney, Kunimasa Saitoh, Kento Iizawa, Yukihiro Tsuchida, Masanori Koshiba and Sinha R K 2008 *Opt. Lett.* **33** 2431
[7] Ben Salem A, Cherif R and Zghal M 2011 *PIERS Proceedings*, Marrakesh, Morocco, March 20–23, Russia
[8] Bhawana Dabas and Sinha R K 2010 *Opt. Commun.* **283** 1331
[9] Gopinath J, Soljacic M, Ippen E, Fuflyigin V, King W and Shurgalin M 2004 *J. Appl. Phys.* **96** 6931
[10] Wang H L, Yang A J and Leng Y X 2014 *Laser Physics* **24** 035101
[11] Wang H L, Yang A J and Leng Y X 2013 *Laser Physics* **23** 075102
[12] Wang H L, Yang A J and Leng Y X 2013 *Chin. Phys. B* **22** 074208
[13] Wang H L, Leng Y X and Xu Z Z 2009 *Chin. Phys. B* **18** 1
[14] Wu Y 2013 *Laser Phys. Lett.* **10** 095107
[15] Jonathan Hu, Curtis R Menyuk and Brandon Shaw L 2010 *Opt. Lett.* **35** 2907-2909
[16] Yan Z, Wen J G, Zhao C J, Wang W L and Wang Y L 2015 *International Conference on Information Sciences, Machinery, Materials and Energy* (ICISMME 2015)
[17] Sourabh Roy and Partha Roy Chaudhuri 2015 *Opt. Commun.* **282** 3448
[18] Lenz G, Zimmermann J, Katsufuji T, Lines M E, Hwang H Y, Spalter S, Slusher R E and Cheong S W 2000 *Opt. Lett.* **25** 254